

NATIONAL INSTITUTE FOR FUSION SCIENCE**3D Electromagnetic Theory of ICRF Multi Port
Multi Loop Antenna**

V.L. Vdovin and I.V. Kamenskij

(Received - Oct. 28, 1996)

NIFS-479

Jan. 1997

**RESEARCH REPORT
NIFS Series**

This report was prepared as a preprint of work performed as a collaboration research of the National Institute for Fusion Science (NIFS) of Japan. This document is intended for information only and for future publication in a journal after some rearrangements of its contents.

Inquiries about copyright and reproduction should be addressed to the Research Information Center, National Institute for Fusion Science, Nagoya 464-01, Japan.

**3D ELECTROMAGNETIC THEORY of ICRF MULTI PORT
MULTI LOOP ANTENNA**

**Vdovin V.L.,^{*)}
National Institute for Fusion Science**

**Kamenskij I.V.
Canberra National University, Australia**

CONTENT:

Abstract

- I. Introduction. Indexes and definitions
 - II. Expressions for EM fields in antenna regions I,II
 - III. Fields in regions III,IV
 - IV. Divertor region (region V)
 - V. Boundary conditions on plasma surface
 - VI. Fields matching at antenna mouth ($r=b$)
 - VII. Fields matching at sub recess mouthes
 - VIII. Linear system of equations
 - IX. Total antenna impedance and impedance matrix
 - 9.1 *Loops are deeply in sub recesses*
 - 9.2 *Loops are outside of sub recesses*
 - X. Radial power flux
- Appendix

^{*)}On leave from Kurchatov Institute, Moscow

ABSTRACT

In this report the theory of three dimensional antenna in Ion Cyclotron Resonance Frequency (ICRF) is developed for a plasma with circular magnetic surfaces. The multi loop antenna is located in ITER several ports. Circular plasma and antenna geometry provides new important tools to account for: 1) right loading antenna impedance matrix calculation urgently needed for a matching of RF generator with an antenna; 2) right calculation of an antenna toroidal and poloidal excited spectra because the DIFFRACTION, refraction and REFLECTION effects for the Fast Waves (FW) are in FIRST time are included self consistently in 3D ICRF antenna - plasma treatment; 3) right calculation of RF power deposition profiles because self consistently found 3D antenna - plasma FW excited spectra in non slab plasma model are important ones in a weakly dissipated plasma for Fast Waves (even for ITER parameters).

In the developed theory multi loop antennae are located in several ITER ports with arbitrary relative toroidal and poloidal positions. It gives great flexibility of investigation possibility for production of an optimal ICRF antenna directivity in conditions of limited toroidal space in a reactor port and a possibility to control width of excited FW k - spectra to control RF power deposition profiles into a plasma. The above theory allows to calculate RF losses on a Faraday screen bars.

In the model developed each loop is located in a special individual recess in a tokamak port to control in some extent mutual coupling between loops through a vacuum port region and simultaneously to support the Faraday screen bars. The theory developed accounts for two options for poloidal loops: to be located INSIDE of each sub recess (with a smaller mutual loops coupling) and to be located OUTSIDE of each sub recess (more closely to plasma) with an increased antenna loading resistance. Radial antenna loops feeders are taken into account as well.

The MULTI PORT structure of the theory gives another important tool to control mutual coupling of loops: it is possible to locate one port just near another one with, for example, only two loops in each sub PORT just simulating continuous conducting boundary between several loops (besides of sub recess walls). Another possibility is to simulate extended toroidal port size to improve an antenna directivity. The information about plasma properties comes into antenna theory through plasma surface impedance matrix Y_{mm} and is calculated separately by fast MINTOR2 code described in Part A. According to theory developed the ANPORT code has been written. The first runs indicated strong mutual loops coupling of ITER now designed antenna. The work is under progress.

Key Words: Antenna, ICRF, port, multi-loop, current drive, plasma heating, ITER, tokamak, code, plasma, impedance matrix

I. INTRODUCTION. INDEXES and DEFINITIONS

In following theory of multi port, multi loop antennae (each poloidal loop is located in an individual sub-recess) we define meanings of several indexes and clusters of indexes, along with some another termins.

j - number of a port

l - “local” number of sub recess in a port

i -th “global” (over all ports) number of sub loop and a number of EM fields, excited by i -th sub loop.

Numeration of sub loops: since 1st port, from left to right, and from bottom to a top (see Fig. 1ap).

m - poloidal number of a mode in a plasma/SOL,

$$m = m_{\min, \dots, -1, 0, 1, \dots, m_{\max}}$$

n - toroidal number of a mode in a plasma/SOL

$$n = n_{\min, \dots, -1, 0, 1, \dots, n_{\max}}$$

M - poloidal number of a mode in ports/sub recesses

$$M = 0, 1, \dots, M_{\max}$$

N - toroidal number of a mode in port (regions III, IV),

$$N = 1, 2, 3, \dots, N_{\max}$$

η - toroidal number of a mode in a sub recess (regions I, II)

$$\eta = 1, 2, 3, \dots, \eta_{\max}$$

“CLAUSTER” indexes:

$I = \{j M N\}$ - “global” number of mode in a port

(over all ports)

$J = \{j l M \eta\}$ - “global” mode number in a “sub recess”

II. EXPRESSIONS for EM FIELDS in ANTENNA REGIONS I, II

Here are given the expressions for electromagnetic fields in j -th port in sub recess regions I and II (see Fig.1). The components of electrical field, poloidal E_φ and radial E_r , satisfying to the boundary conditions on an antenna conducting walls and back plate, are as follows (in l -th

$$E_\varphi(r, \varphi, z) = \sum_i \sum_l \Theta_l(\varphi, z) \sum_M \cos[\bar{M}(\varphi - \varphi_j^0)] \sin[k_\eta(z - z_{jl}^0)]$$

$$x(-ik_0)\{p_\eta [A_{j\lambda M\eta} J_{\overline{M}}'(p_\eta r) + B_{j\lambda M\eta} Y_{\overline{M}}'(p_\eta r)] + F_{j\lambda M\eta}(r)\} \quad (2.1)$$

The toroidal wave magnetic field is given by

$$B_z(r, \varphi, z) = \sum_i \sum_{M, \eta} \cos[\overline{M}(\varphi - \varphi_j^0)] \sin[k_\eta(z - z_j^0)] \\ x p_\eta^2 \{A_{j\lambda M\eta} J_{\overline{M}}(p_\eta r) + B_{j\lambda M\eta} Y_{\overline{M}}(p_\eta r) + F_{j\lambda M\eta}(r)\} \quad (2.2)$$

The radial electrical field is:

$$E_r(r, \varphi, z) = \sum_i \sum_{M, \eta} \sin[\overline{M}(\varphi - \varphi_j^0)] \sin[k_\eta(z - z_j^0)] \\ x \left(-\frac{ik_0}{r}\right) \{\overline{M} [A_{j\lambda M\eta} J_{\overline{M}}(p_\eta r) + B_{j\lambda M\eta} Y_{\overline{M}}(p_\eta r)] + G_{j\lambda M\eta}(r)\} \quad (2.3)$$

In the above formulas (2.1)-(2.3) J_M and Y_M are the Bessel functions of first kind of fractional \underline{M} order. The function $\Theta_l(\varphi, z)$ is

$$\Theta_l(\varphi, z) = \begin{cases} 1 & \text{inside of l-th sub recess} \\ 0 & \text{outside of l-th sub recess} \end{cases}$$

The coefficients A,B to be found we will supply by upper indexes I,II inside of of sub recess (I) and outside it (II):

$$\underline{A}, \underline{B}^I, \quad r > s$$

$$\underline{A}, \underline{B} =$$

$$\underline{A}, \underline{B}^{II}, \quad r \leq s$$

The functions F(r) and G(r) describe the role of radial feeders of current carrying loops:

$$F_{jIM\eta_i}(r) = \frac{4\pi\bar{J}_{iM\eta}}{cP_\eta^2} \bar{M} u_{M\eta}(r) \theta_s(r) \Delta_{ijl} \quad (2.4)$$

$$G_{jIM\eta_i}(r) = \frac{4\pi\bar{J}_{iM\eta}}{cP_\eta^2} (\bar{M}^2 u_{M\eta}(r) + 1) \theta_s(r) \Delta_{ijl} \quad (2.5)$$

Here $\bar{J}_{iM\eta}$ is radially independent constant in Fourier component of radial antenna excitation current:

$$J_{r,iM\eta}(r) = \frac{1}{r} \bar{J}_{iM\eta}$$

The function $u(r)$ is a special solution of ordinary second order inhomogeneous differential equation and it together with constants $\bar{J}_{iM\eta}$ is described in Appendix. The fractional order of Bessels depends on poloidal space extension angle of a port Ψ_p :

$$\bar{M} = \frac{\pi M}{\Psi_p}, \quad M=0,1,2,\dots$$

The function $\theta_s(r)$ discriminates regions inside and outside of the sub recess:

$$\theta_s(r) = \begin{cases} 1, & r \geq s \\ 0, & r < s \end{cases}$$

The subscripted flag Δ_{ijl} discriminates if i -th antenna loop belongs or not to $\{j,1\}$ -th sub recess:

$$\Delta_{ijl} = \begin{cases} 1, & \text{if } i\text{-th loop} \in \{j,1\} \text{ sub recess} \\ 0, & \text{if not} \end{cases}$$

The sub recess toroidal wave number is given by

$$k_\eta = \frac{\pi\eta}{L_r}, \quad \eta=1,2,3,\dots$$

where L_r is toroidal width of a sub recess. Another definitions for wave numbers are given as

$$p_\eta^2 = k_0^2 - k_\eta^2, \quad k_0 = \omega / c, \quad p_\eta = \sqrt{|p_\eta^2|}$$

Here ω is a generator frequency, and c is speed of light.

The boundary condition at the back plate in each recess

$$\vec{E}^I(r = r_w) = 0$$

and jump of a magnetic field across antenna's poloidal loop if $s > r_s$

$$[B_z^II - B_z^I]_{r=s} = \frac{4\pi}{c} j_\varphi$$

together with continuity of poloidal electric field at a loop

$$[E_\varphi^II - E_\varphi^I]_{r=s} = 0$$

result in system of linear equations:

$$A_{J_1}^{II} = \gamma_{M\eta}^I B_{J_1}^{II} + Q_{J_1}^{II}$$

$$A_{J_1}^I = \gamma_{M\eta}^I B_{J_1}^I + Q_{J_1}^I$$

$$A_{J_1}^{II} = A_{J_1}^I + q_{J_1}^I$$

$$B_{J_1}^{II} = B_{J_1}^I + q_{J_1}^{II}$$

where for brevity we used collective index $J = \{j|lM\eta\}$. Here

$$\gamma_{M\eta}^I = -\frac{Y_{\bar{M}}'(p_\eta r_w)}{J_{\bar{M}}'(p_\eta r_w)}, \quad Q_{J_1}^I = -\frac{F_{J_1}^I(r_w)}{p_\eta J_{\bar{M}}'(p_\eta r_w)}$$

$$Q_{J_1}^{II} = Q_{J_1}^I + q_{J_1}^I - \gamma_{M\eta}^I q_{J_1}^{II}$$

$$q_{J_1}^I = w_\eta p_\eta s [R_1 Y_{\bar{M}}'(p_\eta s) - R_2 Y_{\bar{M}}(p_\eta s)]$$

$$q_{j_i}'' = -w_\eta p_\eta s [R_1 J_{\bar{M}}'(p_\eta s) - R_2 J_{\bar{M}}(p_\eta s)]$$

$$R_1 = \frac{4\pi}{c p_\eta^2} J_{iM\eta}^\varphi + F_{j_i}(s), \quad R_2 = \frac{F_{j_i}'(s)}{p_\eta}$$

(w_η is given in Appendix).

If $i \notin \{j, 1\}$ or $i \in \{j, 1\}$, but $s < r_s$, then $\{q^I, q^{II}\} = 0$.

III. FIELDS in REGIONS III, IV

In port regions outside of sub recesses area, $b \leq r \leq r_s$, the fields in any tokamak port, satisfying to boundary conditions, have the following expressions:

$$E_\varphi(r, \varphi, z) = \sum_i \sum_j \Theta_j(\varphi, z) \sum_{M,N} \cos[\bar{M}(\varphi - \varphi_j^0)] \sin[k_N(z - z_j^0)] \quad (9)$$

$$x(-k_0) \{ p_N [A_{jMNi} J_{\bar{M}}'(p_N r) + B_{jMNi} Y_{\bar{M}}'(p_N r)] + F_{jMNi}'(r) \}$$

The toroidal wave magnetic field component in j-th port is:

$$B_z(r, \varphi, z) = \sum_i \sum_{M,N} \cos[\bar{M}(\varphi - \varphi_j^0)] \sin[k_N(z - z_j^0)] \\ x p_N^2 \{ A_{jMNi} J_{\bar{M}}(p_N r) + B_{jMNi}(p_N r) + F_{jMNi}(r) \} \quad (3.2)$$

Radial electrical wave field in that region is as

$$E_r(r, \varphi, z) = \sum_i \sum_{M,N} \sin[\bar{M}(\varphi - \varphi_j^0)] \sin[k_N(z - z_j^0)] \\ x \left(-\frac{ik_0}{r}\right) \{ \bar{M} [A_{jMNi} J_{\bar{M}}(p_N r) + b_{jMNi} Y_{\bar{M}}(p_N r)] + G_{jMNi}(r) \}$$

The function $\Theta_j(\varphi, z)$ keeps the poloidal electrical field to be zero outside of j-th port:

$$\Theta_j(\varphi, z) = \begin{cases} 1 & \text{inside of j-th port} \\ 0 & \text{elsewhere} \end{cases}$$

0 outside of it

The coefficients A,B have the indexes to discriminate regions outside of the loop (IV) and inside of the loop if last one is moved outside of sub recess more closely to the plasma (see Fig.1):

$$A,B = \begin{cases} A^I, B^{III}, & r > s \\ A^V, B^{IV}, & r \leq s \end{cases}$$

In above formulas the toroidal wave number in a port (outside of sub recesses) is defined as

$$k_N = \frac{\pi N}{L_p}, \quad N = 1,2,3,..$$

where L_p is a toroidal broadness of a port. The functions $F(r)$ and $G(r)$ are given by

$$F_{jMNi}(r) = \frac{4\pi \bar{J}_{iMN}}{c p_N^2} \bar{M} u_{MN}(r) \theta_s(r) \Delta_{ij}$$

$$G_{jMNi}(r) = \frac{4\pi \bar{J}_{iMN}}{c p_N^2} (\bar{M}^2 u_{MN}(r) + 1) \theta_s(r) \Delta_{ij}$$

$$\Delta_{ij} = \begin{cases} 1 & i \in \text{to } j\text{-th port} \\ 0 & i \notin \text{to } j\text{-th port} \end{cases}$$

In the case of poloidal loops being protruded outside of sub recess region, i.e. $s < r_s$, we account for jump of wave magnetic field across of a loop and continuity of poloidal electric field:

$$\left[B_z^{IV} - B_z^{III} \right]_{r=s} = \frac{4\pi}{c} j_\varphi, \quad \text{if } s < r_s$$

$$\left[E_\varphi^{IV} - E_\varphi^{III} \right]_{r=s} = 0$$

These two last conditions create the new linear equations:

$$A_{jMNi}^{IV} = A_{jMNi}^{III} + q_{jMNi}^{III}$$

$$B_{jMNi}^{IV} = B_{jMNi}^{III} + q_{jMNi}^{IV}$$

where

$$q_{jMNi}^{III} = w_N p_N s \{ \tilde{R}_1 Y_M'(p_N r) - \tilde{R}_2 Y_M(p_N r) \}$$

$$q_{jMNi}^{IV} = -w_N p_N s \{ \tilde{R}_1 J_M'(p_N s) - \tilde{R}_2 J_M(p_N s) \}$$

If $i \notin j$ or $s > r_s$ then $q^{III}, q^{IV} = 0$.

IV. DIVERTOR REGION (region V)

In this section we consider region between bulk plasma ($r=a$) and a first wall ($r=b$) and name that as divertor region (region V). In this region poloidal electric field excited by all loops (current global index is "I") over all ports we expand in Fourier series over plasma toroidal and poloidal harmonics (m,n):

$$E_\varphi(r, \varphi, z) = \sum_i \sum_{m,n} e^{im\varphi + ik_n z} (-ik_0 p_n) \{ A_{mni}^V J_m'(p_n r) + B_{mni}^V Y_m'(p_n r) \}$$

$$B_z(r, \varphi, z) = \sum_i m \sum_{mn} e^{im\varphi + inz} p_n^2 \{ A_{mni}^V J_m(p_n r) + B_{mni}^V Y_m(p_n r) \}$$
(4)

Here toroidal plasma wave number is given as

$$k_n = \frac{n}{R}, \quad n=0, \pm 1, \pm 2, \dots$$

$$p_n^2 = k_0^2 - k_n^2, \quad p_n = \sqrt{|p_n^2|}$$

V. BOUNDARY CONDITIONS AT PLASMA SURFACE

At plasma vacuum boundary we require the continuity of poloidal electric field and the continuity of a toroidal component of wave magnetic field:

$$E_{\phi}^{\text{plasma}} = E_{\phi}^{\text{vacuum}}, \quad B_z^{\text{plasma}} = B_z^{\text{vacuum}} \quad (5.1)$$

In our previous report [1] we developed the procedure for calculation of wave fields in inhomogeneous plasma. For our antenna electromagnetic characteristics (antenna impedance matrix, spectrum of excited waves, Ohmic losses on the Faraday screen, etc.) to be found it will be sufficient to make use the plasma surface impedance [1]:

$$Y_{mn} = \left[\frac{E_{\phi mn}}{B_{z mn}} \right]_{r=a-0} \quad (5.2)$$

Then from (5.1) and (5.2) one has

$$A_{mn}^V = \gamma_{mn}^V B_{mn}^V, \quad \tilde{Y}_{mn} = i \frac{p_n^2}{k_0 p_n} Y_{mn}$$

$$\gamma_{mn}^V = - \frac{\tilde{Y}_{mn} Y_m(p_n a) - Y_m'(p_n a)}{\tilde{Y}_{mn} J_m(p_n a) - J_m'(p_n a)} \quad (5.3)$$

From formulas (5.3) we see that coefficient γ^V is closely related with reflection coefficient from plasma.

VI. FIELDS MATCHING AT ANTENNA MOUTH ($r = b$)

Now we start important procedure of fields matching at an antenna (port) mouth. We stress that in many ITER related 2D full wave codes the fields are matched term by term in Fourier series, so speaking about port antenna but dealing with an antenna located in SOL region. In presented theory we are doing real in port antenna solution by matching TOTAL em fields at an antenna mouth. We equate total fields at $r = b$, multiply equality by $\exp(-im\varphi - ik_n z)$ and integrate first wall surface. Schematically it looks like:

$$\int_{-\pi}^{\pi} d\varphi \int_{-\pi R}^{\pi R} dz e^{-im\varphi - ik_n z} [E_{\phi}^V = E_{\phi}^{IV}]_{r=b}$$

The same we are doing for the magnetic fields B_z , integrating over j-th port:

$$\int_{\text{OVER-J-TH-PORT}} d\varphi dz \cos[\overline{M}(\varphi - \varphi_j^0)] \sin[k_N(z - z_j^0)] \left[B_z^V = B_z^{IV} \right]_{r=b}$$

This results in important system of linear equations:

$$\sum_I \{G_{II'} A_{I_i}^{III} + H_{II'} B_{I_i}^{III}\} = D_{I_i} \quad (6.1)$$

where

$$D_{I_i} = q_{I_i}^{III} J_{\overline{M}}(p_N b) + q_{I_i}^{IV} Y_{\overline{M}}(p_N b) - \\ - \sum_I T_{II'} \{q_{I_i}^{III} J_{\overline{M}}'(p_N b) + q_{I_i}^{IV} Y_{\overline{M}}'(p_N b)\},$$

The coefficients G and H are given by

$$G_{II'} = T_{II'} J_{\overline{M}}'(p_N b) - \delta_{II'} J_{\overline{M}}(p_N b)$$

$$H_{II'} = T_{II'} Y_{\overline{M}}'(p_N b) - \delta_{II'} Y_{\overline{M}}(p_N b)$$

As above, the prime at the head of Bessels {J,Y} means differentiation over its arguments, and δ_{ij} is Kroneker function.

In the above integration we made use an orthogonality of trigonometric functions. The real information about plasma, chamber and ports sizes are comes through T coefficient:

$$T_{II'} = \frac{P_N}{\pi^2 R \Delta_M L_p \Psi_p P_N^2} \sum_{mn} R_{mn} \alpha_{jMm} \alpha_{j'M'm}^* \beta_{jNn} \beta_{j'N'n}^*$$

$$R_{mn} = \frac{p_n^2}{p_n} \frac{\gamma_{mn}^V J_m(p_n b) + Y_m(p_n b)}{\gamma_{mn}^V J_m'(p_n b) + Y_m'(p_n b)}$$

$$\Delta_M = \begin{cases} 2, & M=0 \\ 1, & M \neq 0 \end{cases}$$

The reflective wave amplitude at an antenna/port mouth is given by

$$B_{mm}^I = \frac{1}{4\pi^2 R p_n [\gamma_{mn}^V J_m'(p_n b) + Y_m'(p_n b)]} \\ \times \sum_{j, M, N} \alpha_{jMm}^* \beta_{jNn}^* p_N [A_{jMN}^{IV} J_M'(p_N b) + B_{jMN}^{IV} Y_M'(p_N b)]$$

The integration geometrical coefficients α_{jMm} , β_{jNn} are given in Appendix.

VII. FIELDS MATCHING at SUB RECESSES MOUTHES

Inside of a j -th port we must also to match em fields at sub recesses openings at $r = r_s$. We again multiply the equalities of total em fields by trigonometric functions and integrate in toroidal direction over a port size L_p and over a sub recess size L_r to make use orthogonality of trgonometric functions:

$$\int_{z_j^0}^{z_j^0 + L_p} dz \sin[k_N(z - z_j^0)] [E_\varphi^II = E_\varphi^III]_{r=s}$$

$$\int_{z_j^0}^{z_j^0 + L_r} dz \sin[k_\eta(z - z_j^0)] [B_z^II = B_z^III]_{r=s}$$

Making use the expressions for the fields from previous sections one gets a continuation of linear equations for unknown coefficients for the em fields:

$$\sum_N (V_{MNN'} A_{jMN'}^{III} + W_{MNN'} B_{jMN'}^{III}) = U_{jMN'} \quad (7.1)$$

Here

$$V_{MNN'} = T_{MNN'} J_M'(p_N r_s) - \frac{L_p}{2} p_N J_M'(p_N r_s) \delta_{NN'}$$

$$W_{MNN'} = T_{MNN'} Y_M'(p_N r_s) - \frac{L_p}{2} p_N Y_M'(p_N r_s) \delta_{NN'}$$

The right hand side of Eq . (7.1) includes also a contribution of radial antenna feeders (through the function F):

$$U_{jMNi} = \frac{L_p}{2} F'_{jMNi}(r_s) - \sum_N T_{MNN'} F_{jMN'i}(r_s) + \sum_{i\eta} \mu_{iN\eta} \{ p_\eta^2 R_{M\eta} [F_{jM\eta}(r_s) + Q_{jM\eta}^{II} J_{\bar{M}}(p_\eta r_s)] - p_\eta Q_{jM\eta}^{II} J_{\bar{M}}'(p_\eta r_s) - F'_{jM\eta i}(r_s) \}$$

Matrix T is given by

$$T_{MNN'} = \frac{2}{L_r} p_N^2 \sum_i \sum_\eta (\mu_{iN\eta} \mu_{iN'\eta} R_{M\eta})$$

where

$$R_{M\eta} = \frac{p_\eta}{p_\eta^2} \cdot \frac{\gamma_{M\eta}^I J_{\bar{M}}'(p_\eta r_s) + Y_{\bar{M}}'(p_\eta r_s)}{\gamma_{M\eta}^I J_{\bar{M}}(p_\eta r_s) + Y_{\bar{M}}(p_\eta r_s)} .$$

The coefficients $\mu_{iN\eta}$ are given in Appendix.

The coefficient B^{II} is expressed as:

$$B_{j_i}^{II} = \frac{1}{\gamma_{M\eta}^I J_{\bar{M}}(p_\eta r_s) + Y_{\bar{M}}(p_\eta r_s)} \{ -F_{j_i}(r_s) - Q_{j_i}^{II} J_{\bar{M}}(p_\eta r_s) + \frac{2}{L_r p_\eta^2} \sum_N \mu_{iN\eta} p_\eta^2 [A_{i_i}^{III} J_{\bar{M}}(p_N r_s) + B_{i_i}^{III} Y_{\bar{M}}(p_N r_s) + F_{i_i}(r_s)] \}$$

This completes preparatory work for solving antenna problem on a computer.

VIII. LINEAR SYSTEM OF EQUATIONS

The derived linear equations (6.1) and (7.1) we combine in a compact system. For the brevity we use “cluster” index $I = \{j, M, N\}$.

$$\sum_I P_{II'} B_{I'I}^{III} = \bar{D}_{I'} - \bar{U}_{I'} \quad (8.1)$$

It means that

$$B_{I'}^{III} = \sum_I P_{II'}^{-1} (\bar{D}_{I'} - \bar{U}_{I'}) \quad (8.2)$$

where

$$P_{II'} = \bar{H}_{II'} - \bar{W}_{MNN'} \delta_{II'} \delta_{MM'}$$

$$\bar{H}_{II'} = \sum_I G_{II'}^{-1} H_{I'I}$$

$$\bar{D}_{I'} = \sum_I G_{II'}^{-1} D_{I'I}$$

$$\bar{W}_{MNN'} = \sum_N V_{MNN'}^{-1} W_{MN^*N'}$$

$$\bar{U}_{jMN'i} = \sum_N V_{MNN'}^{-1} U_{jMN'i}$$

For example, $V_{MNN'}^{-1}$ is inverted over indexes N, N' matrix $V_{MNN'}$. Then we find

$$A_{jMN'i}^{III} = \bar{U}_{jMN'i} - \sum_N \bar{W}_{MNN'} B_{jMN'i}^{III} \quad (8.3)$$

It would be possible to make a solution of the linear system “ideologically simple”, but with greater requirement on “memory”.

IX. TOTAL ANTENNA IMPEDANCE and IMPEDANCE MATRIX

We define total antenna matrix impedance Z through a complex power:

$$P_{RF} = -\frac{1}{2} \int_V \vec{j}^*(\vec{r}) \vec{E}(\vec{r}) dV \equiv \frac{1}{2} Z I_0^2 \quad (9.1)$$

Here I_0 is amplitude of an exciting current in sub loop. (In above definition the multiplier, responsible for averaging of squared current over loop length has not been accounted for simplicity).

The antenna impedance matrix we define as

$$Z_{ii'} = -\int_V \vec{j}_i^*(\vec{r}) \vec{E}_{i'}(\vec{r}) dV \quad (9.2)$$

assuming unit loop current: $I_0 = 1$ SGSM. In Eqs. (9.1), (9.2) integration is performed over volume of excited antenna currents (over the loops). The contribution of radial antenna feeders in an impedance is evaluated by trapezia rules (we recall that “ i ” is a global sub loop number over all ports and recesses).

In following the indexes j, l (j is port number, l is “local” number of a sub recess in a port) are those, that $\Delta_{i,jl} = 1$.

9.1 Loops are deeply in sub recesses

In this case $s > r_s$. Then performing an integration we find:

$$Z_{ii'} = \frac{i}{4} k_0 \Psi_p L_r \left\{ s \sum_1 + \frac{r_w - s}{2} \sum_2 \right\} \quad (9.1.1)$$

Here

$$\sum_1 = \sum_{M\eta} J_{\varphi i M \eta}^* \Delta_M \left\{ P_\eta [A_{j l M \eta}^i \cdot J_{\bar{M}}^i(p_\eta s) + B_{j l M \eta}^i \cdot Y_{\bar{M}}^i(p_\eta s)] + F_{j l M \eta}^i(s) \right\} \quad (9.1.2)$$

$$\begin{aligned} \sum_2 = \sum_{M\eta} \bar{J}_{i M \eta}^* \{ \bar{M} [A_{j l M \eta}^i \cdot \left(\frac{J_{\bar{M}}^i(p_\eta s)}{s} + \frac{J_{\bar{M}}^i(p_\eta r_w)}{r_w} \right) \right. \\ \left. + B_{j l M \eta}^i \cdot \left(\frac{Y_{\bar{M}}^i(p_\eta s)}{s} + \frac{Y_{\bar{M}}^i(p_\eta r_w)}{r_w} \right) \right] \\ \left. + \frac{G_{j l M \eta}^i(s)}{s} + \frac{G_{j l M \eta}^i(r_w)}{r_w} \right\}. \end{aligned} \quad (9.1.3)$$

The above impedance formulas are useful in many respects. For example from (9.1.1) follows that impedances are proportional to poloidal antenna extent Ψ_p .

9.2 Loops are outside of sub recesses

In this case antenna sub loops are moved more closely to plasma to increase an active impedance (loading resistance): $s < r_w$. Direct evaluation of (9.2) gives the impedance matrix:

$$Z_{ii} = \frac{i}{4} k_0 \Psi_p \{ L_p (s \sum_1 + \frac{r_s - s}{2} \sum_2) + L_r \frac{r_w - r_s}{2} \sum_3 \} \quad (9.2.1)$$

The contribution of poloidal RF current to the impedance is given by

$$\sum_1 = \sum_{MN} J_{\varphi MN}^* \Delta_M \{ p_N [A_{jMNi}^{III} J_M'(p_N s) + B_{jMNi}^{III} Y_M'(p_N s)] + F_{jMNi}'(s) \} \quad (9.2.2)$$

Contribution of radial feeders outside of a recess is:

$$\begin{aligned} \sum_2 = \sum_{MN} \bar{J}_{iMN}^* \{ \bar{M} [A_{jMNi}^{III} (\frac{J_M(p_N s)}{s} + \frac{J_M(p_N r_s)}{r_w}) + \\ B_{jMNi}^{III} (\frac{Y_M(p_N s)}{s} + \frac{Y_M(p_N r_s)}{r_s})] + \\ \frac{G_{jMNi}(s)}{s} + \frac{G_{jMNi}(r_s)}{r_s} \} \end{aligned} \quad (9.2.3)$$

Contribution of part radial feeders, located inside of a recess, to the impedance matrix is given by:

$$\begin{aligned} \sum_3 = \sum_{M\eta r} \bar{J}_{iM\eta}^* \{ \bar{M} [A_{jM\eta i}^I (\frac{J_M(p_\eta r_s)}{r_s} + \frac{J_M(p_\eta r_w)}{r_w}) + \\ B_{jM\eta i}^I (\frac{Y_M(p_\eta r_s)}{r_s} + \frac{Y_M(p_\eta r_w)}{r_w})] + \\ \frac{G_{jM\eta i}(r_s)}{r_s} + \frac{G_{jM\eta i}(r_w)}{r_w} \} \end{aligned} \quad (9.2.4)$$

X. RADIAL POWER FLUX

Making use orthogonality eigen functions the radial power flux is expressed in a compact form:

$$\Pi_r = -\frac{c}{8\pi} \int_{-\pi}^{\pi} d\varphi \int_{-\pi R}^{\pi R} r dz \operatorname{Re}[E_\varphi B_z^*] = \sum_{mn} \Pi_{mn}$$

where at a port mouth $r = b$ each Fourier term is given by

$$\Pi_{mn} = \frac{1}{2\omega_n} \omega \pi R \rho_n^2 |B_{mn}^V|^2 \operatorname{Im}(\gamma_{mn}^V) \quad (10.1)$$

Here magnetic field B_{mn}^V is a contribution of all loops of multi port antenna

$$B_{mn}^V = \sum_i B_{mni}^V$$

APPENDIX

1a. BESSEL FUNCTIONS

In this report many times appearing Bessel functions J and Y are understood as:

$$J_\alpha(pr), Y_\alpha(pr) = \begin{cases} J_\alpha(pr), Y_\alpha(pr), & p^2 \geq 0 \\ I_\alpha(pr), K_\alpha(pr), & p^2 < 0 \end{cases}$$

where $I_\alpha(z)$ and $K_\alpha(z)$ are modified Bessel functions

The Wronskian of Bessels has a form:

$$J_\alpha(pr)Y'_\alpha(pr) - J'_\alpha(pr)Y_\alpha(pr) = \frac{1}{w_p pr}$$

where

$$w_p = \begin{cases} \pi/2, & p^2 \geq 0 \\ -1, & p^2 < 0 \end{cases}$$

2a. COEFFICIENTS α_{jMm} , β_{jNn} , $\mu_{jN\eta}$

The coefficient alfa is the integral:

$$\alpha_{jMm} = \int_{\varphi_j^0}^{\varphi_j^0 + \Psi_p} \cos[\overline{M}_M(\varphi - \varphi_j^0)] e^{im\varphi} d\varphi =$$

$$\begin{cases}
\left[-ie^{im\varphi_j^0} [(-1)^M e^{im\Psi_p} - 1] \frac{m}{m^2 - \overline{M}_M^2}, \dots, |m| \neq |\overline{M}_M| \right] \\
= \left\{ \frac{\Psi_p}{2} e^{im\varphi_j^0}, \dots, |m| = |\overline{M}_M| \neq 0 \right. \\
\left. \Psi_p, \dots, m = M = 0 \right.
\end{cases}$$

The coefficient beta is the integral over toroidal wide of a port:

$$\begin{aligned}
\beta_{jNn} &= \int_{z_j^0}^{z_j^0 + L_p} \sin[k_N(z - z_j^0)] e^{ik_n z} dz = \\
&= \begin{cases}
\left[e^{ik_n z_j^0} [(-1)^N e^{ik_n L_p} - 1] \frac{k_N}{k_n^2 - k_N^2}, \dots, |k_n| \neq |k_N| \right] \\
\left\{ i \frac{L_p}{2} e^{ik_n z_j^0}, \dots, k_n = k_N \right. \\
\left. -i \frac{L_p}{2} e^{ik_n z_j^0}, \dots, k_n = -k_N \right.
\end{cases}
\end{aligned}$$

The coefficient mu is integral over toroidal width of l-th sub recess of j-th port:

$$\begin{aligned}
\mu_{lN\eta} &= \int_{z_j^0}^{z_j^0} \sin[k_N(z - z_j^0)] \sin[k_\eta(z - z_{jl}^0)] dz = \\
&= \begin{cases}
\left[\frac{k_\eta}{k_N^2 - k_\eta^2} \{(-1)^N \sin[k_N(z_l^0 + L_\tau)] - \sin[k_N z_l^0]\}, \dots, k_N \neq k_\eta \right] \\
\left\{ \frac{L_\tau}{2} \cos(k_N z_l^0), \dots, k_N = k_\eta \right.
\end{cases}
\end{aligned}$$

where $z_l^0 = l(L_\tau + d_s)$ and d_s is thickness of a sub recess wall in toroidal direction.

3a. FUNCTION U(r)

Presence of radial antenna feeders requires of solution of inhomogeneous differential equation. In cylindrical antenna geometry it is a particular solution of the equation:

$$r^2 u''(r) + ru'(r) + (p^2 r^2 - \bar{M}^2) u = 1$$

where prime means differentiation over r. We find this solution numerically by an expansion $u(r)$ in Teylor series over $t = r/s - 1$ argument near of $t = 0$.

4a. FOURIER COMPONENTS OF SUB LOOP CURRENTS

On Fig. 1ap we scetch antenna mouth how it is seen from a plasma center. In each sub recess are located 2 sub loops (or even one sub loop as an option). The poloidal angle antenna loop and port angle sizes are shown together with coordinates of loop centers in polodal and toroidal directions.

Two operational modes of RF feed are also shown: out phase and sin phase feeds, creating different Fast wave exciting spectra.

For the out phase feed the expressions for Fourier harmonics of excing currents are:

$$J_{\varphi iM\eta} = \frac{e^{i\Phi_i}}{D} J_{\varphi iM} J_{\eta}$$

It is a current in sub peccess. The poloidal current Fourier component in a port region outside of a recess is given by

$$J_{\varphi iMN} = \frac{e^{i\Phi_i}}{D} J_{\varphi iM} J_{iN}$$

In theses formulas Φ_i and D are respectively phase of i-th loop and toroidal wide of a loop.

The "hatted" currents in main text are:

$$\bar{J}_{iM\eta} = \frac{e^{i\Phi_i}}{D} \bar{J}_{iM} J_{\eta}$$

$$\bar{J}_{iMN} = \frac{e^{i\Phi_i}}{D} \bar{J}_{iM} J_{iN}$$

Here

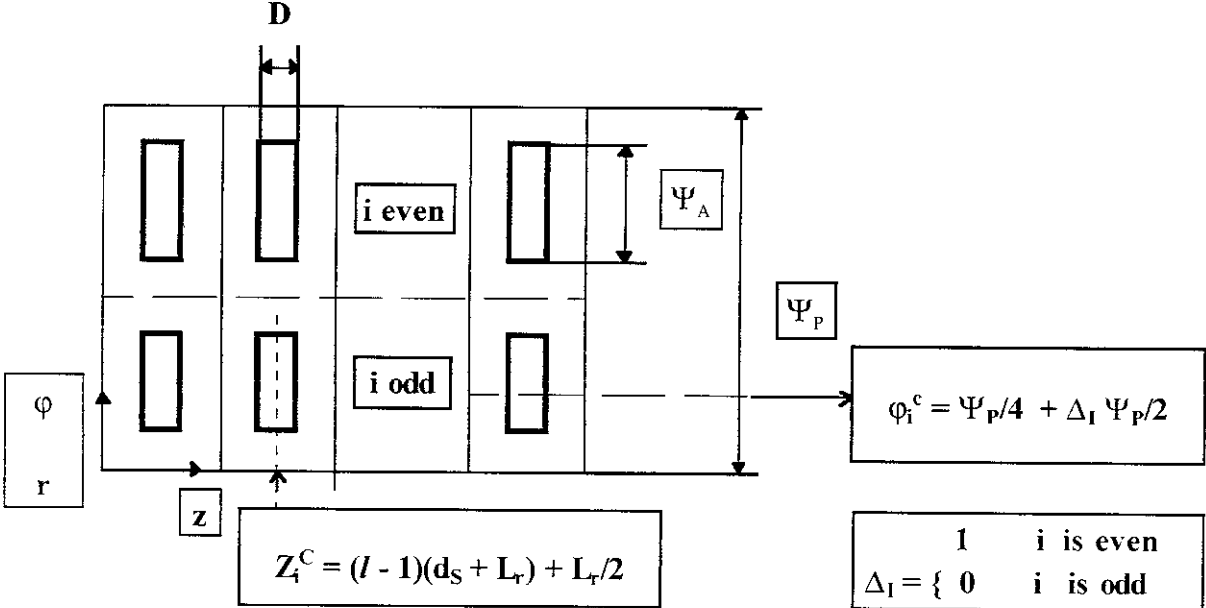
$$J_n = \frac{4}{\pi n} \sin\left(\frac{\pi n}{2}\right) \sin\left(k_n \frac{D}{2}\right)$$

$$J_{in} = \frac{4}{\pi N} \sin(k_N z_i^c) \sin\left(k_N \frac{D}{2}\right)$$

For out phase feed

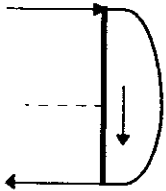
$$\tilde{J}_M = \frac{4}{\Psi_p} \cos(\bar{M} \varphi_i^c) \cos\left(\beta s \frac{\Psi_a}{2}\right) \sin\left(\bar{M} \frac{\Psi_a}{2}\right)$$

Fig.1ap. FOURIER COMPONENTS OF SUB LOOP CURRENTS



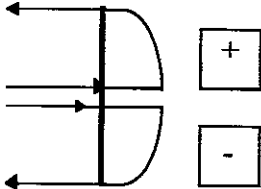
RF FEED of SUB LOOP

out phase feed



$j_\phi \sim \cos[\beta s(\phi - \phi_i^c)]$

sinphase RF feed



Recent Issues of NIFS Series

- NIFS-439 K. Ida, K. Kondo, K. Nagasaki, T. Hamada, H. Zushi, S. Hidekuma, F. Sano, T. Mizuuchi, H. Okada, S. Besshou, H. Funaba, Y. Kurimoto, K. Watanabe and T. Obiki,
Dynamics of Ion Temperature in Heliotron-E; Sep. 1996 (IAEA-CN-64/CP-5)
- NIFS-440 S. Morita, H. Idei, H. Iguchi, S. Kubo, K. Matsuoka, T. Minami, S. Okamura, T. Ozaki, K. Tanaka, K. Toi, R. Akiyama, A. Ejiri, A. Fujisawa, M. Fujiwara, M. Goto, K. Ida, N. Inoue, A. Komori, R. Kumazawa, S. Masuzaki, T. Morisaki, S. Muto, K. Narihara, K. Nishimura, I. Nomura, S. Ohdachi, M. Osakabe, A. Sagara, Y. Shirai, H. Suzuki, C. Takahashi, K. Tsumori, T. Watari, H. Yamada and I. Yamada,
A Study on Density Profile and Density Limit of NBI Plasmas in CHS; Sep. 1996 (IAEA-CN-64/CP-3)
- NIFS-441 O. Kaneko, Y. Takeiri, K. Tsumori, Y. Oka, M. Osakabe, R. Akiyama, T. Kawamoto, E. Asano and T. Kuroda,
Development of Negative-Ion-Based Neutral Beam Injector for the Large Helical Device; Sep. 1996 (IAEA-CN-64/GP-9)
- NIFS-442 K. Toi, K.N. Sato, Y. Hamada, S. Ohdachi, H. Sakakita, A. Nishizawa, A. Ejiri, K. Narihara, H. Kuramoto, Y. Kawasumi, S. Kubo, T. Seki, K. Kitachi, J. Xu, K. Ida, K. Kawahata, I. Nomura, K. Adachi, R. Akiyama, A. Fujisawa, J. Fujita, N. Hiraki, S. Hidekuma, S. Hirokura, H. Idei, T. Ido, H. Iguchi, K. Iwasaki, M. Isobe, O. Kaneko, Y. Kano, M. Kojima, J. Koog, R. Kumazawa, T. Kuroda, J. Li, R. Liang, T. Minami, S. Morita, K. Ohkubo, Y. Oka, S. Okajima, M. Osakabe, Y. Sakawa, M. Sasao, K. Sato, T. Shimpo, T. Shoji, H. Sugai, T. Watari, I. Yamada and K. Yamauti,
Studies of Perturbative Plasma Transport, Ice Pellet Ablation and Sawtooth Phenomena in the JIPP T-IIU Tokamak; Sep. 1996 (IAEA-CN-64/A6-5)
- NIFS-443 Y. Todo, T. Sato and The Complexity Simulation Group,
Vlasov-MHD and Particle-MHD Simulations of the Toroidal Alfvén Eigenmode; Sep. 1996 (IAEA-CN-64/D2-3)
- NIFS-444 A. Fujisawa, S. Kubo, H. Iguchi, H. Idei, T. Minami, H. Sanuki, K. Itoh, S. Okamura, K. Matsuoka, K. Tanaka, S. Lee, M. Kojima, T.P. Crowley, Y. Hamada, M. Iwase, H. Nagasaki, H. Suzuki, N. Inoue, R. Akiyama, M. Osakabe, S. Morita, C. Takahashi, S. Muto, A. Ejiri, K. Ida, S. Nishimura, K. Narihara, I. Yamada, K. Toi, S. Ohdachi, T. Ozaki, A. Komori, K. Nishimura, S. Hidekuma, K. Ohkubo, D.A. Rasmussen, J.B. Wilgen, M. Murakami, T. Watari and M. Fujiwara,
An Experimental Study of Plasma Confinement and Heating Efficiency through the Potential Profile Measurements with a Heavy Ion Beam Probe in the Compact Helical System; Sep. 1996 (IAEA-CN-64/C1-5)
- NIFS-445 O. Motojima, N. Yanagi, S. Imagawa, K. Takahata, S. Yamada, A. Iwamoto, H. Chikaraishi, S. Kitagawa, R. Maekawa, S. Masuzaki, T. Mito, T. Morisaki, A. Nishimura, S. Sakakibara, S. Satoh, T. Satow, H. Tamura, S. Tanahashi, K.

- Watanabe, S. Yamaguchi, J. Yamamoto, M. Fujiwara and A. Iiyoshi,
Superconducting Magnet Design and Construction of LHD; Sep. 1996
(IAEA-CN-64/G2-4)
- NIFS-446 S. Murakami, N. Nakajima, S. Okamura, M. Okamoto and U. Gasparino,
Orbit Effects of Energetic Particles on the Reachable β -Value and the Radial
Electric Field in NBI and ECR Heated Heliotron Plasmas; Sep. 1996 (IAEA-
CN-64/CP -6) Sep. 1996
- NIFS-447 K. Yamazaki, A. Sagara, O. Motojima, M. Fujiwara, T. Amano, H. Chikaraishi,
S. Imagawa, T. Muroga, N. Noda, N. Ohyabu, T. Satow, J.F. Wang, K.Y.
Watanabe, J. Yamamoto . H. Yamanishi, A. Kohyama, H. Matsui, O. Mitarai, T.
Noda, A.A. Shishkin, S. Tanaka and T. Terai
Design Assessment of Heliotron Reactor; Sep. 1996 (IAEA-CN-64/G1-5)
- NIFS-448 M. Ozaki, T. Sato and the Complexity Simulation Group,
Interactions of Convecting Magnetic Loops and Arcades; Sep. 1996
- NIFS-449 T. Aoki,
*Interpolated Differential Operator (IDO) Scheme for Solving Partial
Differential Equations*; Sep. 1996
- NIFS-450 D. Biskamp and T. Sato,
Partial Reconnection in the Sawtooth Collapse; Sep. 1996
- NIFS-451 J. Li, X. Gong, L. Luo, F.X. Yin, N. Noda, B. Wan, W. Xu, X. Gao, F. Yin, J.G.
Jiang, Z. Wu., J.Y. Zhao, M. Wu, S. Liu and Y. Han,
Effects of High Z Probe on Plasma Behavior in HT-6M Tokamak; Sep. 1996
- NIFS-452 N. Nakajima, K. Ichiguchi, M. Okamoto and R.L. Dewar,
Ballooning Modes in Heliotrons/Torsatrons; Sep. 1996 (IAEA-CN-64/D3-6)
- NIFS-453 A. Iiyoshi,
Overview of Helical Systems; Sep. 1996 (IAEA-CN-64/O1-7)
- NIFS-454 S. Saito, Y. Nomura, K. Hirose and Y.H. Ichikawa,
*Separatrix Reconnection and Periodic Orbit Annihilation in the Harper
Map*; Oct. 1996
- NIFS-455 K. Ichiguchi, N. Nakajima and M. Okamoto,
Topics on MHD Equilibrium and Stability in Heliotron / Torsatron; Oct.
1996
- NIFS-456 G. Kawahara, S. Kida, M. Tanaka and S. Yanase,
*Wrap, Tilt and Stretch of Vorticity Lines around a Strong Straight Vortex Tube
in a Simple Shear Flow*; Oct. 1996
- NIFS-457 K. Itoh, S.- I. Itoh, A. Fukuyama and M. Yagi,
Turbulent Transport and Structural Transition in Confined Plasmas; Oct.

1996

- NIFS-458 A. Kageyama and T. Sato,
Generation Mechanism of a Dipole Field by a Magnetohydrodynamic Dynamo; Oct. 1996
- NIFS-459 K. Araki, J. Mizushima and S. Yanase,
The Non-axisymmetric Instability of the Wide-Gap Spherical Couette Flow;
Oct. 1996
- NIFS-460 Y. Hamada, A. Fujisawa, H. Iguchi, A. Nishizawa and Y. Kawasumi,
A Tandem Parallel Plate Analyzer; Nov. 1996
- NIFS-461 Y. Hamada, A. Nishizawa, Y. Kawasumi, A. Fujisawa, K. Narihara, K. Ida, A. Ejiri,
S. Ohdachi, K. Kawahata, K. Toi, K. Sato, T. Seki, H. Iguchi, K. Adachi, S. Hidekuma,
S. Hirokura, K. Iwasaki, T. Ido, M. Kojima, J. Koong, R. Kumazawa, H. Kuramoto,
T. Minami, I. Nomura, H. Sakakita, M. Sasao, K.N. Sato, T. Tsuzuki, J. Xu, I. Yamada and
T. Watari,
Density Fluctuation in JIPP T-IIU Tokamak Plasmas Measured by a Heavy Ion Beam Probe; Nov. 1996
- NIFS-462 N. Katsuragawa, H. Hojo and A. Mase,
Simulation Study on Cross Polarization Scattering of Ultrashort-Pulse Electromagnetic Waves; Nov. 1996
- NIFS-463 V. Voitsenya, V. Konovalov, O. Motojima, K. Narihara, M. Becker and B. Schunke,
Evaluations of Different Metals for Manufacturing Mirrors of Thomson Scattering System for the LHD Divertor Plasma; Nov. 1996
- NIFS-464 M. Pereyaslavets, M. Sato, T. Shimozuma, Y. Takita, H. Idei, S. Kubo, K. Ohkubo and
K. Hayashi,
Development and Simulation of RF Components for High Power Millimeter Wave Gyrotrons; Nov. 1996
- NIFS-465 V.S. Voitsenya, S. Masuzaki, O. Motojima, N. Noda and N. Ohyabu,
On the Use of CX Atom Analyzer for Study Characteristics of Ion Component in a LHD Divertor Plasma; Dec. 1996
- NIFS-466 H. Miura and S. Kida,
Identification of Tubular Vortices in Complex Flows; Dec. 1996
- NIFS-467 Y. Takeiri, Y. Oka, M. Osakabe, K. Tsumori, O. Kaneko, T. Takanashi, E. Asano, T.
Kawamoto, R. Akiyama and T. Kuroda,
Suppression of Accelerated Electrons in a High-current Large Negative Ion Source; Dec. 1996
- NIFS-468 A. Sagara, Y. Hasegawa, K. Tsuzuki, N. Inoue, H. Suzuki, T. Morisaki, N. Noda, O.
Motojima, S. Okamura, K. Matsuoka, R. Akiyama, K. Ida, H. Idei, K. Iwasaki, S. Kubo, T.
Minami, S. Morita, K. Narihara, T. Ozaki, K. Sato, C. Takahashi, K. Tanaka, K. Toi and I.
Yamada,

Real Time Boronization Experiments in CHS and Scaling for LHD; Dec. 1996

- NIFS-469 V.L. Vdovin, T. Watari and A. Fukuyama,
3D Maxwell-Vlasov Boundary Value Problem Solution in Stellarator Geometry in Ion Cyclotron Frequency Range (final report); Dec. 1996
- NIFS-470 N. Nakajima, M. Yokoyama, M. Okamoto and J. Nührenberg,
Optimization of M=2 Stellarator; Dec. 1996
- NIFS-471 A. Fujisawa, H. Iguchi, S. Lee and Y. Hamada,
Effects of Horizontal Injection Angle Displacements on Energy Measurements with Parallel Plate Energy Analyzer; Dec. 1996
- NIFS-472 R. Kanno, N. Nakajima, H. Sugama, M. Okamoto and Y. Ogawa,
Effects of Finite- β and Radial Electric Fields on Neoclassical Transport in the Large Helical Device; Jan. 1997
- NIFS-473 S. Murakami, N. Nakajima, U. Gasparino and M. Okamoto,
Simulation Study of Radial Electric Field in CHS and LHD; Jan. 1997
- NIFS-474 K. Ohkubo, S. Kubo, H. Idei, M. Sato, T. Shimosuma and Y. Takita,
Coupling of Tilting Gaussian Beam with Hybrid Mode in the Corrugated Waveguide; Jan. 1997
- NIFS-475 A. Fujisawa, H. Iguchi, S. Lee and Y. Hamada,
Consideration of Fluctuation in Secondary Beam Intensity of Heavy Ion Beam Probe Measurements; Jan. 1997
- NIFS-476 Y. Takeiri, M. Osakabe, Y. Oka, K. Tsumori, O. Kaneko, T. Takanashi, E. Asano, T. Kawamoto, R. Akiyama and T. Kuroda,
Long-pulse Operation of a Cesium-Seeded High-Current Large Negative Ion Source; Jan. 1997
- NIFS-477 H. Kuramoto, K. Toi, N. Haraki, K. Sato, J. Xu, A. Ejiri, K. Narihara, T. Seki, S. Ohdachi, K. Adati, R. Akiyama, Y. Hamada, S. Hirokura, K. Kawahata and M. Kojima,
Study of Toroidal Current Penetration during Current Ramp in JIPP T-IIU with Fast Response Zeeman Polarimeter; Jan. 7, 1997
- NIFS-478 H. Sugama and W. Horton,
Neoclassical Electron and Ion Transport in Toroidally Rotating Plasmas; Jan. 1997
- NIFS-479 V.L. Vdovin and I.V. Kamenskij,
3D Electromagnetic Theory of ICRF Multi Port Multi Loop Antenna; Jan. 1997